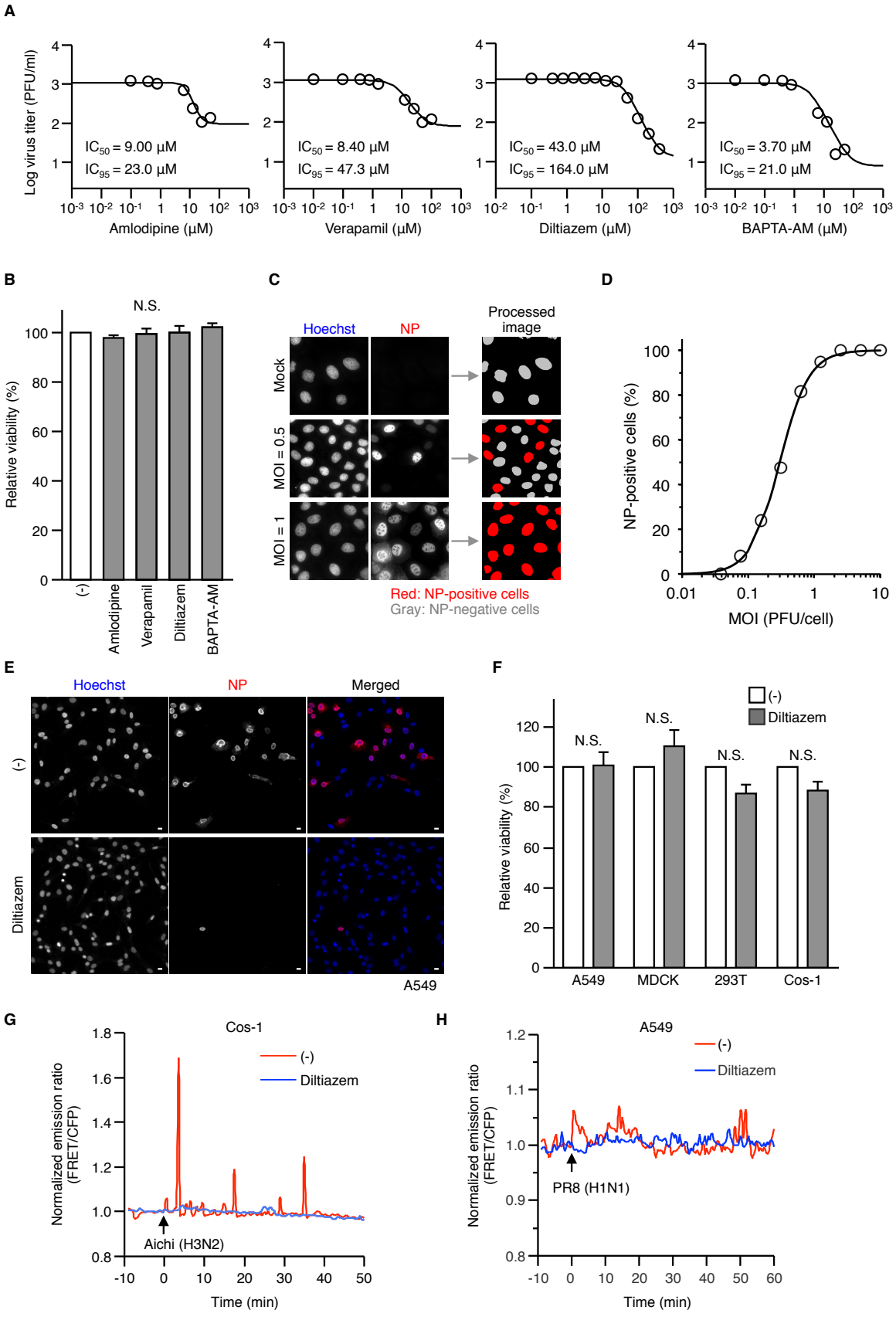
A
Log virus titer (PFU/ml)
IC50 = 9.00 μM
IC95 = 23.0 μM
Amlodipine (μM)
IC50 = 8.40 μM
IC95 = 47.3 μM
Verapamil (μM)
IC50 = 43.0 μM
IC95 = 164.0 μM
Diltiazem (μM)
IC50 = 3.70 μM
IC95 = 21.0 μM
BAPTA-AM (μM)
B
N.S.
Relative viability (%)
(-)
Amlodipine
Verapamil
Diltiazem
BAPTA-AM
C
Hoechst
NP
Processed image
Mock
MOI = 0.5
MOI = 1
Red: NP-positive cells
Gray: NP-negative cells
D
NP-positive cells (%)
MOI (PFU/cell)
E
Hoechst
NP
Merged
(-)
Diltiazem
A549
F
(-)
Diltiazem
N.S.
Relative viability (%)
A549
MDCK
293T
Cos-1
G
Cos-1
(-)
Diltiazem
Normalized emission ratio (FRET/CFP)
Aichi (H3N2)
Time (min)
H
A549
(-)
Diltiazem
Normalized emission ratio (FRET/CFP)
PR8 (H1N1)
Time (min)

Figure S1. Pharmacological Inhibition of VDCCs Suppresses IAV Infection and IAV-induced Ca^{2+} Oscillations, related to Figure 1.

(**A**) Replication of PR8 in the absence or presence of inhibitors at indicated concentrations was determined by an MDCK cell plaque assay. PFU, plaque-forming units.

(**B**) MDCK cells were cultured in the absence or presence of the inhibitors (amlodipine, 25 μM; verapamil, 50 μM; diltiazem, 200 μM; BAPTA-AM, 25 μM) for 48 h, the number of living cells was determined with crystal violet assay, and relative viability to untreated cells was calculated and plotted. Data are means ± s.e.m. (n = 3). N.S., not significant as calculated by one-way ANOVA.

(**C**) Flowchart of immunofluorescence-based infection assay. MDCK cells were infected with IAV for 4 h, fixed and permeabilized. The cells were then incubated with anti-NP antibodies, followed by further incubation with AlexaFluor594-conjugated secondary antibodies. Nuclei were visualized by staining with Hoechst 33342. Images were acquired with a wide-field fluorescence microscope and analyzed with the use of the "Multi-wavelength cell scoring" module of MetaMorph software.

(**D**) The percentage of NP-positive cells was plotted against MOI, and data were fitted to the hill equation: $y = 100 / \{1 + (c / x)^n\}$, with the use of the least-squares method. Note that the results obtained by immunofluorescence-based infection assay and plaque assay were clearly correlated with each other.

(**E**) Representative images showing the effect of diltiazem on PR8 infection in A549 cells as evaluated with an immunofluorescence-based assay (related to **Figure 1C**). Note that few NP-positive cells are apparent in the presence of diltiazem. Bar, 10 μm.

(**F**) Viability of indicated cell lines in the absence or presence of 200 μM diltiazem for 6 h was determined and plotted. Data are means ± s.e.m. (n = 3). N.S., not significant as calculated by Student's t test.

(**G**, **H**) Cos-1 cells (**G**) or A549 cells (**H**) expressing YC3.60 were treated (or not) with 200 μM diltiazem or sialidase (5 mU/ml) for 30 min and then monitored by dual-emission fluorescence microscopy with exposure to Aichi (**G**) or PR8 (**H**) at time 0. Representative traces for the FRET/CFP emission ratio are shown.

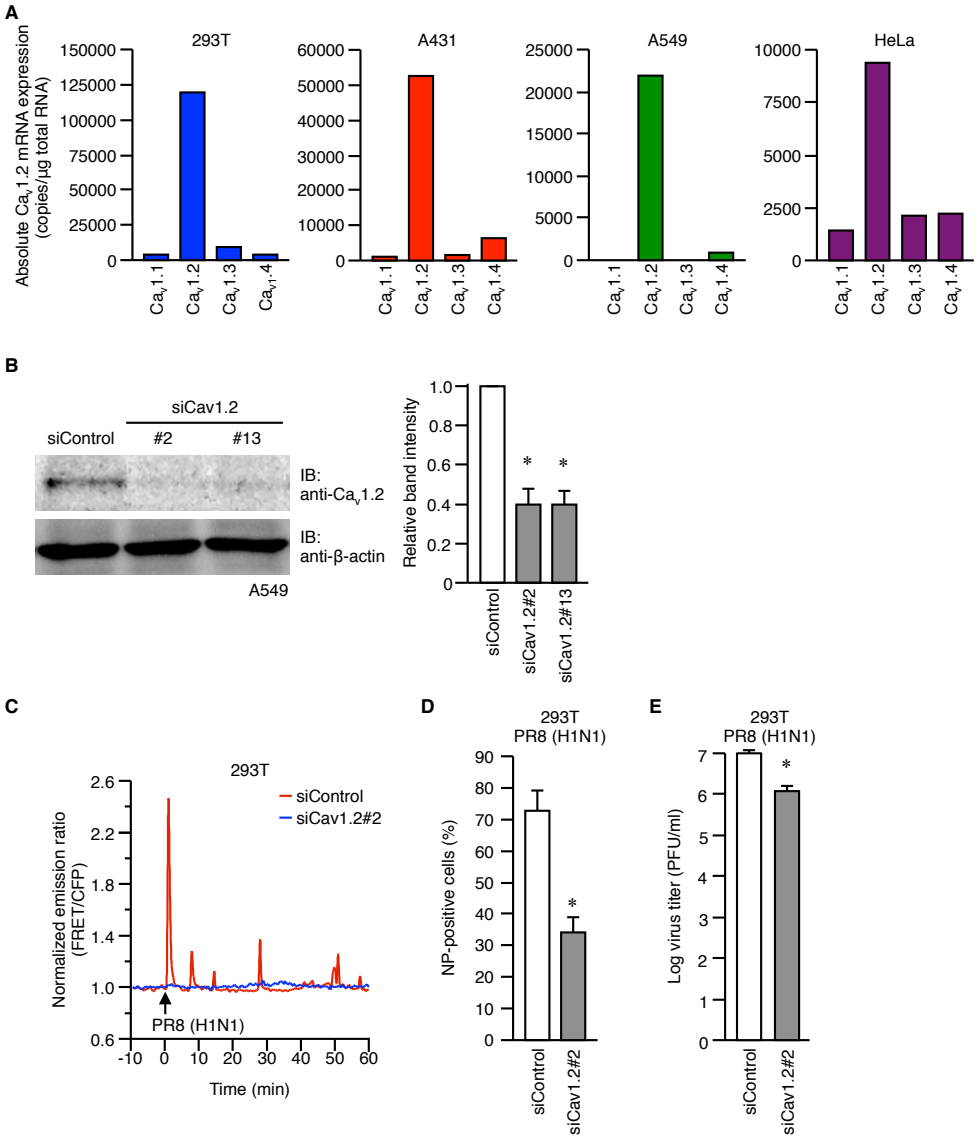

Figure S2. Knockdown of $Ca_v1.2$ Inhibits IAV-Induced Ca^{2+} Oscillations and Virus Infection, related to Figure 2.

(**A**) Total RNA isolated from the indicated cell lines was subjected to reverse transcription (RT) and quantitative polymerase chain reaction (qPCR) analysis. To obtain the calibration curves of $Ca_v1.1$, $Ca_v1.2$, $Ca_v1.3$ and $Ca_v1.4$, plasmids encoding the target sequence from each mRNA were also subjected to qPCR. The copy number of each Ca^{2+} channel was then determined by extrapolation from the curve.

(**B**) A549 cells were transfected for 72 h with an siRNA specific for $Ca_v1.2$ mRNA (siCav1.2#2 or #13) or with a scrambled siRNA (siControl) as a control. The cells were then subjected to immunoblot (IB) analysis with antibodies to $Ca_v1.2$ or to β-actin (loading control) (left panel). The relative expression level of $Ca_v1.2$ normalized by that of β-actin was determined by densitometry (right panel). Data are means ± s.e.m. ($n = 3$). *$P < 0.005$ versus control cells, as calculated by one-way ANOVA with Dunnett's post-test.

(**C**) 293T cells were transfected first for 48 h with the indicated siRNAs and then for 24 h with an expression vector for YC3.60. The cells were then monitored by dual-emission fluorescence microscopy with exposure to PR8 at time 0. Representative traces for the FRET/CFP emission ratio are shown.

(**D**) 293T cells transfected for 72 h with siCav1.2#2 or siControl were exposed to PR8 for 4 h and then subjected to an immunofluorescence-based infection assay. Data are means ± s.e.m. ($n = 3$). *$P = 0.0051$ versus control cells, as calculated by Student's *t* test.

(**E**) 293T cells were transfected for 72 h with siCav1.2#2 or siControl, exposed to PR8 for 48 h, and subjected to an MDCK cell plaque assay. Data are means ± s.e.m. ($n = 4$). *$P = 0.0027$ versus control cells, as calculated by Student's *t* test.

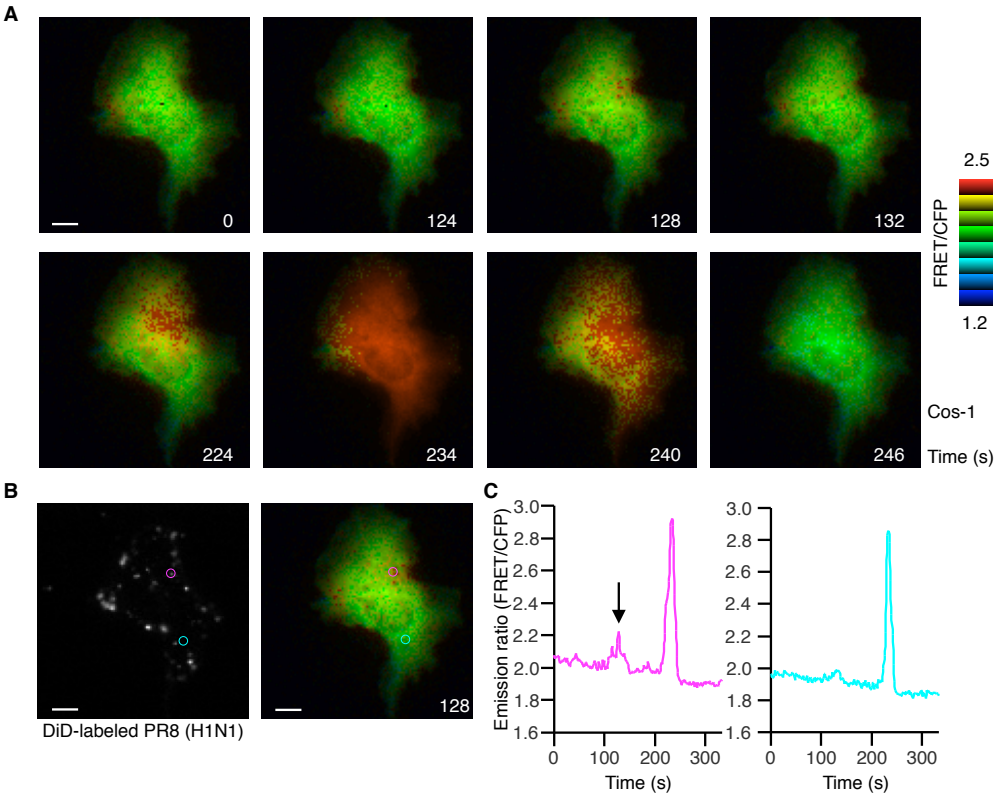
A
0
124
128
132
224
234
240
246
2.5
FRET/CFP
1.2
Cos-1
Time (s)
B
128
DiD-labeled PR8 (H1N1)
C
Emission ratio (FRET/CFP)
3.0
2.8
2.6
2.4
2.2
2.0
1.8
1.6
0
100
200
300
Time (s)
D
A/Puerto Rico/8/34 H1N1
HA2
HA0 (Virus)
HA1
EHA2
Transmembrane
566
1
328
509
HA-His
HA1
EHA2
Foldon
6×His
551
E
FLAG (Alexa488)
CAAX (Sirius)
FLAG-Cav1.2 I-II
FLAG-Cav1.2 III-IV
Normalized surface expression (fold of the I-II fragment)
N.S.
1.2
1.0
0.8
0.6
0.4
0.2
0
I-II
III-IV
Surface/total ratio (fold of the I-II fragment)
0.4
0.3
0.2
0.1
F
CFP-Cav1.2 III-IV - + +
HA-His - + +
Sialidase - - +
IP: anti-GFP
IB: anti-His
IB: anti-Cav1.2
Relative band intensity
*
Sialidase - +

Figure S3. HA of IAV Binds to $Ca_v1.2$ in A Sialylation-Dependent Manner, related to Figure 3.
(**A-C**) DiD-labeled PR8 was allowed to adsorb to YC3.60-expressing Cos-1 cells for 60 min on ice. The cells were then monitored by time-lapse, multidimensional fluorescence microscopy at 37°C. FRET/CFP ratio images were generated to represent FRET efficiency, and the upper and lower limits of the ratio range are indicated. Bar, 10 μm (**A**). A representative image for the DiD channel, in which signals indicate virus adsorption sites, is shown in **B**. Magenta and blue circles indicate a virus adsorption and non-adsorbed site, respectively. Traces for the FRET/CFP emission ratio at the regions indicated by the colored circles in **B** are shown in **C**. The arrow indicates an increase in $[Ca^{2+}]_i$ at a virus adsorption site.
(**D**) Schematic representation of domain structures for wild-type HA of PR8 and a 6×His-tagged form of HA (HA-His) used for co-immunoprecipitation assays.
(**E**) 293T cells expressing Flag-tagged fragments of $Ca_v1.2$ were fixed with 3% paraformaldehyde and subjected to immunofluorescence staining. Representative confocal images are shown. Based on fluorescence images of Sirius-CAAX, total cell area and cell membrane area were determined, and fluorescence intensities in these regions were respectively plotted. Data are means ± s.e.m. (n = 21). N.S., not significant as calculated by Student's t test.
(**F**) 293T cells expressing CFP-tagged fragment III-IV of $Ca_v1.2$ and HA-His were exposed (or not) to sialidase for 30 min and then subjected to immunoprecipitation and immunoblot analysis as indicated. Quantitative data for co-immunoprecipitated HA-His are means ± s.e.m. (n = 4). *P = 0.00036 versus nontreated cells, as calculated by Student's t test.

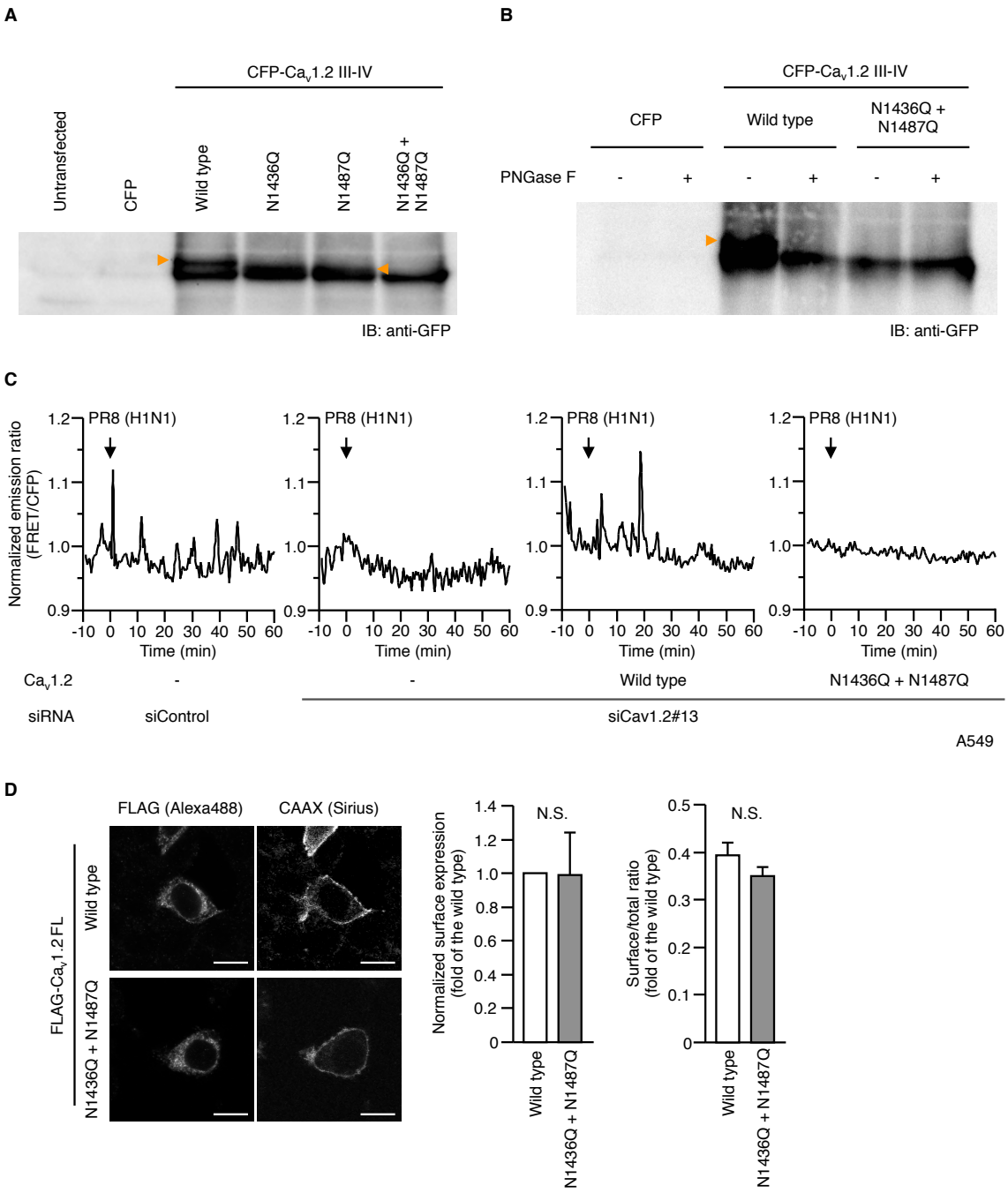

Figure S4. Glycosylation of $Ca_v1.2$ at N1436 or N1487 Is Critical for IAV-Induced Ca^{2+} Oscillations, related to Figure 4.

(**A**, **B**) Immunoblot analysis of fragment III-IV of $Ca_v1.2$ and its glycosylation-deficient mutants expressed in 293T cells that were either left untreated (**A**) or treated with PNGase F (25 U/μl) for 30 min as indicated (**B**) before lysate preparation. Arrowheads indicate glycan-bound forms of the fragment III-IV of $Cav_{1.2}$.

(**C**) A549 cells transfected with $Ca_v1.2$ or control siRNAs were further transfected with expression vectors for wild-type or glycosylation-deficient mutant forms of $Ca_v1.2$ as well as for YC3.60. The cells were exposed to PR8 at time 0 and monitored by dual-emission fluorescence microscopy. Representative traces for the FRET/CFP emission ratio are shown.

(**D**) 293T cells were transfected with an expression vector for the wild type or a glycosylation-deficient mutant of $Ca_v1.2$ and then subjected to immunofluorescence staining. Representative confocal images are shown. Total and cell-surface expression of the wild-type and mutant $Ca_v1.2$ were determined as in Figure S3E, and plotted. Data are means ± s.e.m. (n = 19). N.S., not significant as calculated by Student's t test.

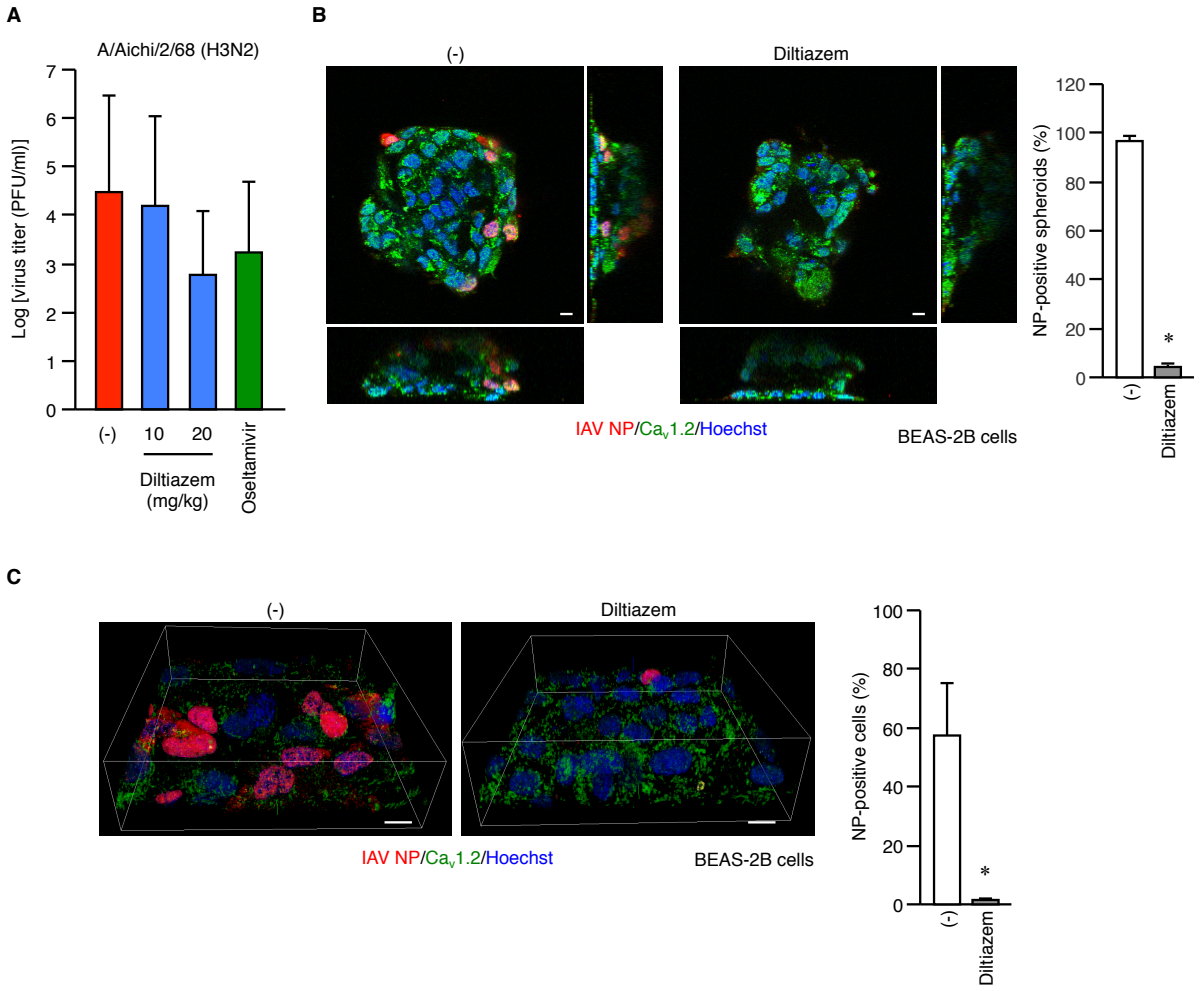

Figure S5. Diltiazem Inhibits IAV Replication *In Vivo* and *Ex Vivo*, related to Figure 6.
(**A**) The effect of prophylactic administration of diltiazem on the replication of the IAV strain Aichi was evaluated by plaque assay in nasal lavage fluid and was compared with that of oseltamivir. Data are means ± s.e.m. ($n > 5$). $P = 0.024$ as calculated by one-way ANOVA.
(**B, C**) Human bronchial epithelial (BEAS-2B) cells were cultured on (**B**) or in (**C**) Matrigel. After formation of spheroids (**B**) or an epithelial monolayer (**C**), the cells were incubated in the absence or presence of diltiazem for 2 h, and were then exposed to PR8 for 4 h at an MOI of 1 PFU/cell. The specimens were fixed, subjected to immunofluorescence staining with antibodies to $Ca_v1.2$ and IAV NP, and observed under confocal microscopy. A series of sections, covering from the top to the bottom of cells, were obtained, and representative *xy*, *yz*, and *xz* images of spheroids (**B**) and reconstructed 3D images of monolayers (**C**) are shown. Quantitative data for infection are means ± s.e.m. (Student's *t* test. $n > 70$)